

## Measurement of Microkelvin Temperature Differences in a Critical-Point Thermostat<sup>1</sup>

R. F. Berg,<sup>2,3</sup> G. A. Zimmerli,<sup>4</sup> and M. R. Moldover<sup>2</sup>

---

The density of a pure fluid near its critical point is extremely sensitive to temperature gradients. In the absence of gravity, this effect limits the fluid's homogeneity. For example, at 0.6 mK above the critical temperature, the microgravity experiment Critical Viscosity of Xenon (CVX) can allow temperature differences no larger than  $0.2 \mu\text{K}$ , corresponding to a gradient of  $10^{-5} \text{K} \cdot \text{m}^{-1}$ . The CVX thermostat, which consists of a thick-walled copper cell contained within three concentric aluminum shells, was designed to achieve such a small temperature gradient. However, asymmetries not included in the thermostat's model could degrade the thermostat's performance. Therefore we measured the temperature gradient directly with a miniature commercial thermoelectric cooler consisting of 66 semiconductor thermocouples. We checked the results with a half-bridge consisting of two matched thermistors. The measurement was made along a thin-walled stainless-steel cell whose conductance was much lower than that of the copper cell, thus "amplifying" the temperature differences by a factor of 60. When the thermostat was controlled at a constant temperature, the steel cell's static temperature difference was  $5 \pm 1 \mu\text{K}$ . (The value inferred for the copper cell is  $0.08 \mu\text{K}$ .) Ramping the thermostat's temperature at a rate of  $1 \times 10^{-5} \text{K} \cdot \text{s}^{-1}$  increased the temperature difference to 0.36 mK. These results demonstrate the feasibility of achieving extremely low temperature gradients.

---

**KEY WORDS:** critical point; temperature control; temperature gradients; thermostat.

---

<sup>1</sup> Paper presented at the Thirteenth Symposium on Thermophysical Properties, June 22–27, 1997, Boulder, Colorado, U.S.A.

<sup>2</sup> Physical and Chemical Properties Division, National Institute of Standards and Technology, Gaithersburg, Maryland 20899, U.S.A.

<sup>3</sup> To whom correspondence should be addressed.

<sup>4</sup> Engineering Services Division, NYMA, Incorporated, Brook Park, Ohio 44142, U.S.A.

## 1. INTRODUCTION

The present thermostat is a type of enclosure thermostat [1] frequently used for critical point experiments (e.g., see Refs. 2–4). Its construction and operation are briefly described first; further details are given in Ref. 5. The thermostat's ability to achieve small temperature differences within the sample cell was estimated by calculations associated with identified asymmetries. The magnitudes of some asymmetries were well-known, such as the thermal lag at the copper cell's sapphire window which occurred while cooling the cell. The magnitudes of others were based on a conservative assumption, such as a 10% imbalance between the left and the right heaters of the thermostat's inner shell. Our uncertainty about the thermostat's actual asymmetries motivated the present measurements.

In addition to validating the thermostat's performance, the present measurements demonstrate the usefulness of a thermopile for measuring small temperature differences near room temperature.

## 2. APPARATUS

### 3.1. Thermostat Construction

In normal operation, the CVX sample is held in a cell whose thick copper walls greatly reduce the temperature differences imposed by the surrounding thermostat. As shown in Fig. 1, the thermostat consisted of three concentric cylindrical shells. To guarantee small temperature gradients at the cell, the shells and their end caps were made from 6-mm-thick aluminum, with a radial gap of 13 mm between shells. The large radial gap and the stiff, glass-filled polycarbonate spacers made the design mechanically robust and insensitive to errors of design and construction. The 38-mm separation between end caps allowed easy installation of the cell and its wiring. The weak coupling resulting from the large gaps increased the thermostat's response time to more than 1 h. This was acceptable, however, because the thermostat's response time was less than the sample's internal response time near the critical point.

The thermostat's construction began with the attachment of a control thermistor and a pair of thin film heaters to each shell. The heaters were glued around the outer circumference near both ends of the shell, and the thermistor was sealed by thermally conductive epoxy into a hole in the shell's wall underneath the heater. Next, the shells and spacers were bolted together into a rigid structure. Finally, wiring was added to connect the thermistors, heaters, and cell.

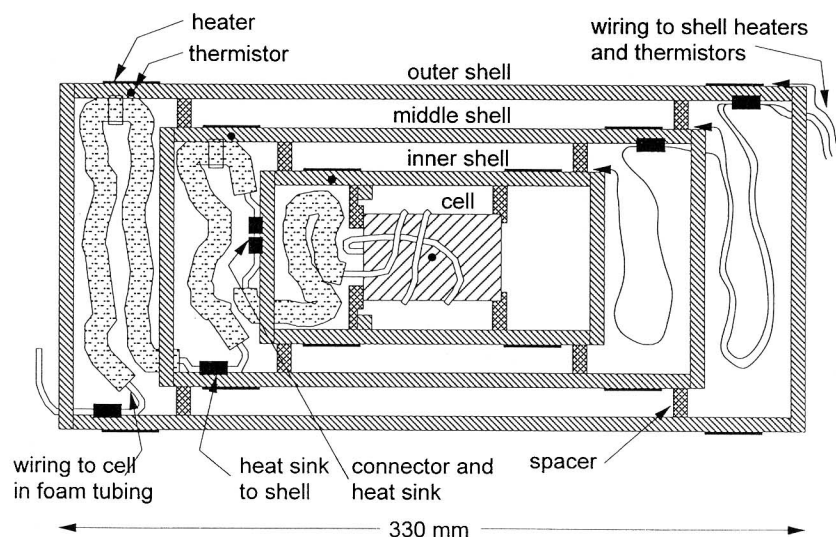


**Fig. 1.** Schematic drawing of the copper cell installed in the thermostat. Removing the left end caps and disconnecting the cell's wiring at the inner shell's left end cap allowed easy access to the cell.

Slow curing of the epoxy surrounding the copper cell's thermistor caused a drift in the thermistor's resistance at a constant temperature. During the 2 weeks following the thermistor's installation, the cell's apparent temperature drifted approximately  $-4$  mK. Raising the cell's temperature to its upper limit of  $34^{\circ}\text{C}$  for 18 h brought the curing to completion and stopped the drift.

The type and layout of the thermostat's electrical wiring were chosen so that the wiring's thermal conductivity was less than 2% of the total conductivity between shells. The heaters and thermistors were connected by No. 30 (0.26-mm-diameter) copper magnet wire. The thermostat also contained 1-mm-diameter coaxial cable (Alpha 9475)<sup>5</sup> whose main thermal conductance consisted of two No. 30 wires. At each shell, the wiring was thermally grounded by adhesive tape and small clamps. In the gap between the shells' end caps, thermal isolation was achieved by organizing the wiring into large loops which spiraled from one shell to the next. The No. 30 wires were bundled by a single length of PTFE spaghetti, and the coaxial cables

<sup>5</sup> In order to describe materials and experimental procedures adequately, it is occasionally necessary to identify commercial products by manufacturers' name or label. In no instance does such identification imply endorsement by the National Institute of Standards and Technology, nor does it imply that the particular product or equipment is necessarily the best available for the purpose.

were bundled by feeding them through a series of 10 mm diameter polyethylene foam tubes. The spaghetti and foam tubes prevented the wiring loops from touching the interior wall of the surrounding shell. Notches in each shell's end cap allowed the wiring to pass through the end cap.

The wiring's placement allowed easy access to the cell; wiring for the cell was placed in the left end of the thermostat, and wiring for the shells was placed in the right end. At the outer and middle shells, the wiring for the cell was not grounded thermally on the end cap. Instead it passed through the end cap and was grounded on the shell's inner diameter, thus allowing easy removal of the end cap.

## 2.2. Thermostat Operation

At each shell, the temperature of the control thermistors was measured once per 8 s by a resistance bridge. The shell's temperature was controlled by the heater power calculated by a proportional-integral-derivative algorithm. In normal operation, the only heat applied to the copper cell was the thermistor's power of approximately  $1 \mu\text{W}$ . Over a few hours, the rms scatter in the cell's apparent temperature was approximately  $10 \mu\text{K}$ .

The heaters induced temperature differences along the length of each shell. The magnitude of these differences was minimized by controlling the inner shell's temperature only 0.03 K above the middle shell's temperature, which in turn was controlled 0.3 K above the outer shell's temperature. The shape of each shell's temperature distribution was expected to be approximately symmetric about the shell's midplane due to the symmetric placement of the shell heaters. Because each thermistor measured the temperature at one point near the shell's end and not a suitable average over the entire shell, a change in the temperature of the thermostat's environment  $\Delta T_{\text{environment}}$  caused a change in the powers of the inner and middle shells. It also caused a small change in the copper cell's temperature  $\Delta T_{\text{Cu cell}}$ ; the attenuation ratio was  $\Delta T_{\text{Cu cell}}/\Delta T_{\text{environment}} = 4 \times 10^{-5}$ .

## 2.3. Thin-Walled Steel Cell

In order to measure the thermostat's temperature differences, the copper cell was replaced by a special cell made from thin-walled stainless-steel tubing. Its axial thermal conductance  $\kappa_{\text{steel cell}}$  was 103 times smaller than that of the copper cell  $\kappa_{\text{Cu cell}}$ , thus "amplifying" the temperature differences between the cell's ends. If the heat flux through the cell were independent of its conductance, then the temperature difference imposed on the cell by its environment would be inversely proportional to its conductance.

However, the cell's conductance  $\kappa_{\text{steel cell}}$  was comparable to the estimated conductance  $\kappa_{\text{shell-cell}}$  between the inner shell and the cell. Thus, instead of 103, the amplification ratio was approximately

$$\frac{\Delta T_{\text{steel cell}}}{\Delta T_{\text{Cu cell}}} = \frac{\kappa_{\text{steel cell}}^{-1} / (\kappa_{\text{steel cell}}^{-1} + \kappa_{\text{shell-cell}}^{-1})}{\kappa_{\text{Cu cell}}^{-1} / (\kappa_{\text{Cu cell}}^{-1} + \kappa_{\text{shell-cell}}^{-1})} = 60 \quad (1)$$

Figure 2 is a schematic diagram of the assembled cell. Brass flanges were brazed onto both ends of the central stainless-steel tube. The thermopile was installed in the cell's hollow interior by soldering L-shaped copper strips first to the thermopile and then to the inside diameters of the flanges. We used 50:50 indium-tin (118°C) solder. A brass end plate and holding ring was bolted to each flange, and a thermistor was installed with thermal grease into a hole drilled into each flange. The No. 30 copper wire leads (two from the thermopile and three from the thermistors) were wrapped once around the cell's outside diameter and taped down for heat sinking. The cell was installed in the thermostat, and the thermostat was installed in a 1-m-tall aluminum enclosure whose temperature could be controlled via cooling coils glued to its lid [6]. For heat sinking, the connecting wires were taped down for at least 10 cm at each thermostat shell's end plate. For thermal isolation, the wiring between shells was at least 30 cm long, and it was loosely balled to minimize contact with the walls. The wires were brought on a common path out of the cooled enclosure to their respective instruments, with no solder connections or other breaks in the copper wires.

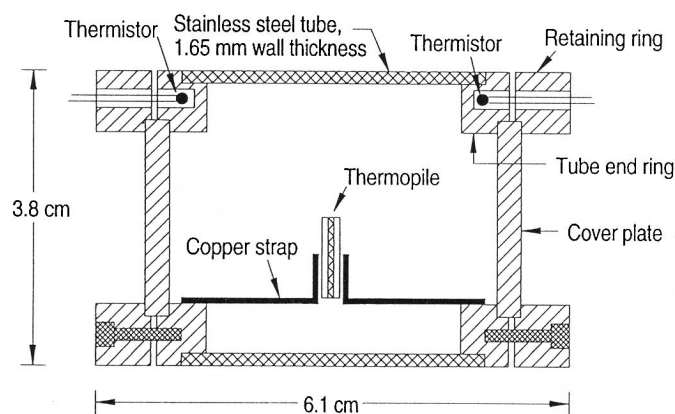


Fig. 2. Schematic drawing of the thin-walled steel cell which replaced the copper cell in the present measurements.

## 2.4. Thermopile

To measure the temperature difference between the ends of the cell, we used a miniature commercial thermoelectric cooler with 66 thermocouples in series (Melcor Model FC0.45-66-05).<sup>5</sup> Its sensitivity to temperature differences, inferred by scaling the manufacturer's performance curves for a similar cooler with 32 thermocouples, was  $0.021 \text{ V} \cdot \text{K}^{-1}$ . The inferred value of the cooler's thermal conductivity was  $0.037 \text{ W} \cdot \text{K}^{-1}$ .

This model was near the optimum size. A model with more thermocouples would have been too large to install in the thin-walled cell. Also, because the cooler's thermal conductivity was directly proportional to the number of thermocouples and already comparable to the thermal conductivity of the connecting copper strips, additional thermocouples would have added little sensitivity to the measurement of the cell's temperature differences. The thermopile's thermal conductance caused the temperature difference  $\Delta T_{\text{pile}}$  across the thermopile to be lower than the difference  $\Delta T_{\text{steel cell}}$  along the cell. The associated correction factor was

$$\frac{\Delta T_{\text{steel cell}}}{\Delta T_{\text{pile}}} = \frac{\kappa_{\text{pile}}^{-1} + \kappa_{\text{strip}}^{-1}}{\kappa_{\text{pile}}^{-1}} = 1.74 \quad (2)$$

where the relevant thermal conductances are listed in Table I. Thus, the effective sensitivity of the thermopile to temperature differences along the cell was estimated at  $0.012 \text{ V} \cdot \text{K}^{-1}$ .

The thermopile's voltage was read by a voltmeter (Keithley Model 182).<sup>5</sup> On the most sensitive scale, its 24 h stability was stated by the manufacturer to be 48 nV, corresponding to  $4 \mu\text{K}$ . We occasionally checked the zero of the voltmeter by shorting the voltmeter's leads. Over the 2 days of measurements, we found slow variations as large as 100 nV, corresponding to variations in  $\Delta T_{\text{steel cell}}$  by as much as  $8 \mu\text{K}$ . The short-term stability of the zero allowed us to measure  $\Delta T_{\text{steel cell}}$  to within  $1 \mu\text{K}$ .

**Table I.** Thermal Conductances of Apparatus Components ( $\text{W} \cdot \text{K}^{-1}$ )

Thermopile	$\kappa_{\text{pile}}$	0.037
Copper strips	$\kappa_{\text{strip}}$	0.050
Thermopile + copper strip assembly	$\kappa_{\text{assembly}}$	0.021
Steel tube	$\kappa_{\text{tube}}$	0.066
Steel tube + thermopile assembly	$\kappa_{\text{steel cell}}$	0.087
CVX copper cell	$\kappa_{\text{Cu cell}}$	9.0
Inner shell to cell	$\kappa_{\text{shell-cell}}$	0.065

### 2.5. Thermistor Bridge

To check the thermopile measurements, we also used a pair of thermistors to measure changes in  $\Delta T_{\text{steel cell}}$ . At each end of the cell, we installed a YSI 44017 thermistor<sup>5</sup> (6 k $\Omega$  at 25°C), and we electrically connected the pair to form a half-bridge. The outer pair of leads was connected across an inductive voltage divider, which was driven by a 0.2-V<sub>rms</sub>, 650-Hz voltage through a 1:1 isolation transformer. The common, inner lead was connected to the input of a lock-in amplifier. The voltage divider's tap was grounded, and its ratio was set to null the bridge's output at a temperature difference near zero. The sensitivity of the thermistor bridge, calculated from the thermistor's dependence on temperature and the output voltage's dependence on the divider's ratio, was  $-446 \text{ V} \cdot \text{K}^{-1}$ .

The thermistor bridge verified the thermopile's sensitivity to changes in  $\Delta T_{\text{steel cell}}$ . However, absolute measurements of  $\Delta T_{\text{steel cell}}$  were prevented by the requirement that the thermistors be calibrated to within a few microkelvins. For unknown reasons, the bridge's output drifted by 0.4 mK per day.

## 3. MEASUREMENTS

### 3.1. Initial Check and Cooldown

The cell's operation was checked on the laboratory bench by placing one end on ice, holding the other end at approximately 30°C, and measuring the resulting temperature difference. After placing the cell in the thermostat, a temperature difference of  $\Delta T_{\text{steel cell}} = -22 \text{ mK}$  was noted. This difference, which persisted for at least 1 h, was consistent with the evaporation of a few milligrams of water remaining from the ice test.

The thermostat was mounted in a Hitchhiker cannister, a cylindrical aluminum enclosure approximately 1 m tall. The enclosure's lid was regulated near 12°C, and temperature differences within the enclosure's interior were approximately 1 K. During the overnight cooldown from room temperature to the test temperature near 17°C, the maximum temperature difference peaked at +11 mK. After 10 h,  $\Delta T_{\text{steel cell}}$  had fallen to below +60  $\mu\text{K}$ . The remaining temperature difference decreased slowly during the next 4 h. Figure 3 and 4 show the time dependence of  $\Delta T_{\text{steel cell}}$ .

### 3.2. Thermistor Heating

No temperature difference was detected due to normal operation, in which 1  $\mu\text{W}$  was dissipated in each thermistor. As a check of the thermal

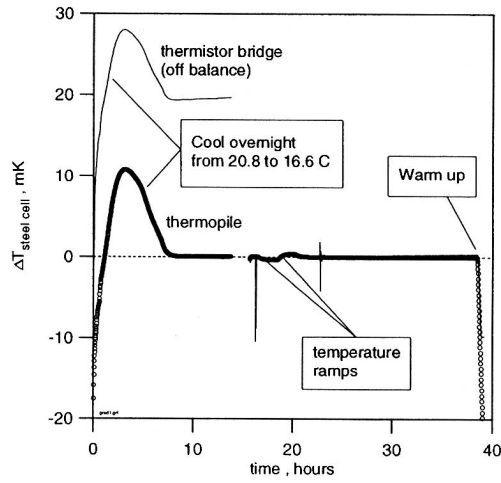


**Fig. 3.** Temperature differences  $\Delta T_{\text{steel cell}}$  measured over 39 h. The thermopile measurements are indicated by circles and the thermistor bridge measurements (with arbitrary offset) by the solid line.

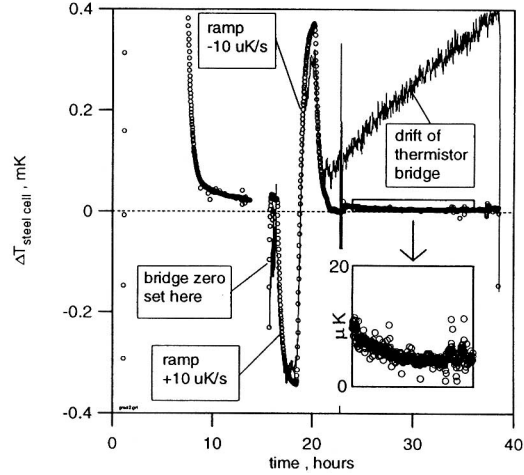


**Fig. 4.** The effects on  $\Delta T_{\text{steel cell}}$  caused by ramping the thermostat's temperature. The thermopile measurements' accuracy is supported by its short-term agreement with the thermistor bridge. The thermistor bridge's drift made it unreliable for long-term measurements.



conductance estimated for the steel cell,  $114 \mu\text{W}$  was applied to the right thermistor. This heating caused a temperature difference of  $\Delta T_{\text{steel cell}} = -538 \mu\text{K}$ , which was consistent with the estimate

$$|\Delta T_{\text{steel cell}}| = \frac{P}{2\kappa_{\text{steel cell}} + \kappa_{\text{shell-cell}}} = 477 \mu\text{K} \quad (3)$$

where  $P$  is the applied power, and  $\kappa_{\text{shell-cell}}$  is the cell-to-inner shell conductance.

### 3.3. Controlled Temperature Ramps

The thermostat's temperature was ramped down at  $-1.00 \times 10^{-5} \text{ K} \cdot \text{s}^{-1}$  then up at  $+1.00 \times 10^{-5} \text{ K} \cdot \text{s}^{-1}$ . As shown in Fig. 4, these ramps caused temperature differences of opposite sign and equal magnitudes of  $355 \mu\text{K}$ , superposed on the background temperature difference of  $15 \mu\text{K}$ .

### 3.4. Constant Temperature

Overnight,  $\Delta T_{\text{steel cell}}$  fell toward a minimum value of approximately  $+(4 \pm 1) \mu\text{K}$ , where the uncertainty accounts for the voltmeter's short-term instability. Measurements of the voltmeter's zero made 10 h later corrected this value to  $+(5 \pm 1) \mu\text{K}$ , the thermostat's ultimate performance with the thin-walled steel cell.

## 4. PREDICTED PERFORMANCE WITH THE COPPER CELL

The temperature difference imposed on the thin-walled steel cell could be characterized by the sum

$$\Delta T_{\text{steel cell}} = \Delta T_0 + \tau_{\text{ramp}} \dot{T} \quad (4)$$

where

$$\Delta T_0 = +5 \mu\text{K} \quad (5)$$

was the temperature difference at a zero ramp rate, and

$$\tau_{\text{ramp}} = \frac{d(\Delta T_{\text{steel cell}})}{d\dot{T}} = -36 \text{ s} \quad (6)$$

characterized the temperature difference caused by ramping the thermostat's temperature at the rate  $\dot{T}$ . A ramp rate of  $\dot{T} = \Delta T_0 / \tau_{\text{ramp}} = -0.14 \mu\text{K} \cdot \text{s}^{-1}$  would be required to double the cell's temperature difference from its value at  $\dot{T} = 0$ .

The thick-walled copper cell's temperature difference can be predicted by dividing the steel cell's temperature difference, Eq. (4), by the factor of 60 from Eq. (2). This prediction does not account for temperature differences produced by thermistor heating and by differential cooling of the cell's components. However, the calculations of these local effects do not have the uncertainties associated with thermostat asymmetries and are of the order of only  $0.1 \mu\text{K}$  [5]. For  $\dot{T} = 0$ , the predicted temperature difference is  $\Delta T_{\text{Cu cell}} = 0.08 \mu\text{K}$ .

#### ACKNOWLEDGMENTS

Bruce Law's emphasis on demonstrations of thermostat performance led to this investigation. The thermostat and its controlling electronics were constructed for the CVX microgravity experiment by a NYMA and ADF team in Cleveland, Ohio. This work was supported by NASA under Contract C32014-C.

#### REFERENCES

1. S. C. Greer, in *Building Scientific Apparatus*, J. H. Moore, C. C. Davis, and M. A. Coplan, eds. (Addison-Wesley, Reading, MA, 1989) p. 524.
2. R. B. Kopelman, R. W. Gammon, and M. R. Moldover, *Phys. Rev. A* **29**:2048 (1984).
3. R. F. Kayser, J. W. Schmidt, and M. R. Moldover, *Phys. Rev. Lett.* **54**:707 (1985).
4. R. F. Berg and M. R. Moldover, *Rev. Sci. Instrum.* **57**:1667 (1986).
5. R. F. Berg and M. R. Moldover, CVX Science Requirements Document 60009-DOC-006 (NASA Lewis Research Center, 1996).
6. A. M. Peddie, Flight instrument specification for the Critical Viscosity of Xenon flight project 60009-DOC-014 (NASA Lewis Research Center, 1996).